Eur. Phys. J. Special Topics **225**, 2173–2188 (2016)

DOI: 10.1140/epjst/e2016-60055-y

THE EUROPEAN PHYSICAL JOURNAL SPECIAL TOPICS

Review

# Magnetotactic bacteria

## Magnetic navigation on the microscale

Stefan Klumpp[1,2,a] and Damien Faivre[3]

[1] Institute for Nonlinear Dynamics, Georg August University Göttingen, Friedrich-Hund-Platz 1, 37077 Göttingen, Germany
[2] Department Theory & Bio-Systems, Max Planck Institute of Colloids and Interfaces, 14424 Potsdam, Germany
[3] Department Biomaterials, Max Planck Institute of Colloids and Interfaces, 14424 Potsdam, Germany

Received 17 February 2016 / Received in final form 19 April 2016
Published online 10 November 2016

**Abstract.** Magnetotactic bacteria are aquatic microorganisms with the ability to swim along the field lines of a magnetic field, which in their natural environment is provided by the magnetic field of the Earth. They do so with the help of specialized magnetic organelles called magnetosomes, vesicles containing magnetic crystals. Magnetosomes are aligned along cytoskeletal filaments to give linear structures that can function as intracellular compass needles. The predominant viewpoint is that the cells passively align with an external magnetic field, just like a macroscopic compass needle, but swim actively along the field lines, propelled by their flagella. In this minireview, we give an introduction to this intriguing bacterial behavior and discuss recent advances in understanding it, with a focus on the swimming directionality, which is not only affected by magnetic fields, but also by gradients of the oxygen concentration.

## 1 Introduction

The magnetic field of the Earth has been key to human navigation for about 1000 years, but it is also used for navigation by animals such as migrating birds and fish [1]. Even the motion of some microorganism is guided by magnetic fields. This behavior, called magnetotaxis, is found in magnetotactic bacteria, a phylogenetically diverse group of aquatic bacteria [2,3]. These bacteria align along magnetic fields with the help of a chain of organelles containing magnetic nanoparticles (magnetosomes), which acts as a compass needle, and swim along the field lines with the help of their flagella.

Magnetotactic bacteria were first described in 1963 by Bellini who isolated and characterized bacteria that followed a magnetic field from various water samples [4]. However, his reports, written in Italian, remained largely unknown. Magnetotactic

[a] e-mail: stefan.klumpp@phys.uni-goettingen.de

bacteria were established as a field of research following their independent discovery by Blakemore 12 years later [5], soon after which the physical nature of the intracellular compass was established [6]. Since then, magnetotactic bacteria have attracted the interest of microbiologists, materials scientists and physicists alike. Today, research on magnetotactic bacteria is a multidisciplinary quest that encompasses several interconnected lines of research. Magnetotactic bacteria provide a model system for compartmentalization and intracellular structure formation in bacterial cells [2,3] and pose some intriguing questions related to their evolution [7]. Moreover, they can be used as a microbial model system for biomineralization, the controlled formation of mineral material in a biological organism [3]. In particular, an understanding how they control shape and size of the magnetic nanoparticles is expected to lead to improvements in the synthesis of such particles in the lab [8]. From a physics perspective, they provide ideal model systems to study how generic physical fields (the magnetic fields) work together with specific biological control mechanisms: Importantly, magnetism provides new biological functions, but also imposes new constraints that the cells have to deal with.

In this minireview, we will focus on magnetotactic bacteria as microswimmers that respond to directional clues and that may be steered with external fields. After a general description of the morphology of these cells and their magnetic apparatus as well as their propulsion mechanism, we will specifically discuss the alignment of the bacteria and their trajectories with the magnetic field as well as their movements in magnetic fields and oxygen gradients. We also give a brief outlook towards synthetic magnetic microswimmers for which magnetotactic bacteria serve as inspiration. For a broad overview of research on magnetotactic bacteria, we refer to Refs. [2,3,9–11].

## 2 Magnetotactic bacteria

In the following, we give a description of the main features of a magnetotactic bacterium. Before doing so, we want to emphasize that magnetotactic bacteria are a diverse group, both morphologically and phylogenetically, and that all aspects of cellular structure described below vary considerably between species of magnetotactic bacteria. Cells come in various shapes: round (cocci), rod-shaped, spirilla, even multicellular. They show a wide variety of magnetosome numbers, particle sizes and particle shapes. Some species have a single chain, some multiple chains. While the best studied magnetotactic bacteria have magnetite ($Fe_3O_4$) nanoparticles [6], some species have been found to use greigite ($Fe_3S_4$) instead [12]. Likewise, the motility apparatus can display various organizations such as a single flagellum or a bundle of flagella at one pole or two flagella at opposite poles [13]. Furthermore, flagella can have different organizations with respect to the magnetosome chain.

Here we will focus on the case of the Magnetospirilla, which are the best studied magnetotactic bacteria. The magnetospirilla (specifically *M. gryphiswaldense* MSR-1 [14] and *M. magneticum* AMB-1) have become somewhat of a standard in the field because they were among the first that could be cultured in the lab and because genetic tools are available enabling mechanistic studies based on mutants. Figure 1 shows an idealized sketch of such a bacterium as well as a representative electron microscopy image of several cells of *M. gryphiswaldense*.

A typical magnetospirillum cell is about three microns long, with a chain of $\sim 20$ magnetosomes extending along the long axis of the cell and two flagella, one at each cell pole. The magnetosome chain is about $1\,\mu$m long and the magnetosomes have a size of $\sim$50 nm in diameter. The magnetosomes are membrane-enclosed compartments that contain a crystalline magnetic nanoparticle, which consists of the iron oxide magnetite, $Fe_3O_4$. In *M. gryphiswaldense* MSR-1, the nanocrystals are

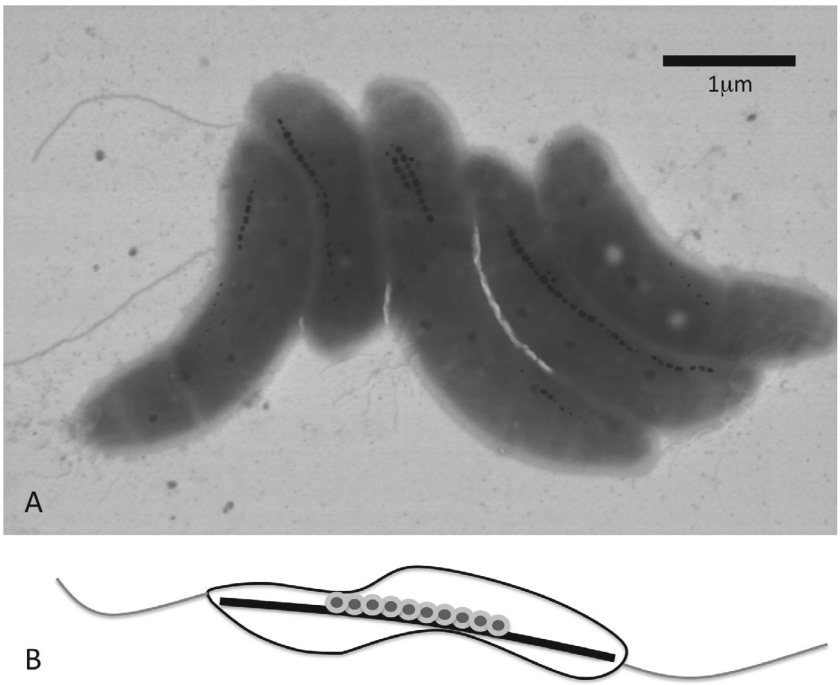


**Fig. 1.** Cellular structure of a magnetotactic bacterium: (A) electron micrograph of *M. gryphiswaldense* cells and (B) schematic sketch of a cell with the magnetosome chain and flagella.

aligned with the ⟨111⟩ direction parallel to the chain axis [15]. Furthermore, this axis is also the easy axis of magnetization and corresponds to the direction of the magnetic moment. Importantly, the size of the magnetite nanoparticles is such that they are single-domain ferrimagnetic and have a permanent magnetic dipole moment with maximal magnetization. Smaller magnetite particles ($\lesssim 35\,\mathrm{nm}$) are superparamagnetic and have no permanent dipole moment, larger particles ($\gtrsim 100\,\mathrm{nm}$) have multiple magnetic domains with different magnetic orientation and thus a lower average magnetization [16]. The dipole moment of a spherical magnetite particle with a diameter of 50 nm is $\simeq 3.1 \times 10^{-17}$ Am$^2$. The dipole-dipole interaction energy is given by

$$E_{12} = -\frac{\mu_0}{4\pi}\frac{1}{r_{12}^3}\left(3\frac{(\mathbf{r}_{12}\cdot\mathbf{m}_1)(\mathbf{r}_{12}\cdot\mathbf{m}_2)}{r_{12}^2} - \mathbf{m}_1\cdot\mathbf{m}_2\right), \tag{1}$$

where $\mathbf{m}_{1,2}$ are the magnetic moments of the two particles and $\mathbf{r}_{12}$ is the vector connecting them. Correspondingly, the attractive force between two such particles with their magnetic moments oriented parallel to $\mathbf{r}_{12}$, which corresponds to the minimal energy configuration, is obtained as

$$F_{12} = -\frac{3\mu_0}{2\pi}\frac{m_1 m_2}{r_{12}^4}. \tag{2}$$

For two magnetite particles of diameter 50 nm, separated only by their surrounding membranes (taken as a gap of 10 nm between the two particles), this gives a force of 44 pN. This is a significant force for intracellular conditions – for example, forces generated by molecular motors and polymerization processes are in the range of

1–10 pN [17]. Thus magnetic forces can be expected to affect intracellular processes, for example during cell division [18,19]. However, the interaction energies and forces are quite sensitive to the distance between the particles and the force decreases quickly if that distance is increased.

Size and shape of the magnetic nanocrystals are tightly controlled by an array of proteins that are associated with the magnetosomes. The genes encoding these proteins are mostly located in one genomic region of 130 kb, the so-called magnetotactic island [20]. A core set of almost 30 genes is conserved between different species of magnetotactic bacteria, but not found in non-magnetic species and appears to be required for the formation and organization of magnetosomes [3,9]. The iron required for the biomineralization process is taken up from the growth medium. If the bacteria are grown in the absence of iron, they form empty magnetosome vesicles without crystals. De novo magnetosome formation can be studied by "feeding" iron to these bacteria [21–23].

The magnetosome particles are attached to a cytoskeletal structure, the so-called magnetosome filament [24,25]. This filament extends along the long axis of the cell. It consists of the protein MamK, a bacterial relative of the eukaryotic cytoskeletal protein actin. Another protein important for the chain structure is MamJ, which is believed to act as a linker between the magnetosomes and the filament (and possibly also between neighboring magnetosomes). One role of the filament is to stabilize the magnetosome chain in the straight configuration [26], but the polymerization and/or depolymerization of the filament may also have dynamic roles in the formation and positioning of the magnetosome chain [23,27].

## 3 Propulsion: The bacterial flagellum

Any bacterial taxis as well as directional motion of synthetic microswimmers requires mechanisms for propulsion and for directionality. As mentioned already, the propulsion of magnetotactic bacteria, just like the swimming of many non-magnetic bacterial species, is based on the rotation of their flagella, long and thin helical filaments driven by a rotary motors in the cell membrane [28]. In the simplest description, bacterial flagella can be understood as rigid helical objects, which locally have cylindrical shape. Propulsion is based on the anisotropic friction of a rod-like particle in a viscous fluid, which experiences larger drag when pulled in a direction perpendicular to its axis than when pulled parallel to its axis (see also Ref. [29]). Due to their chiral structure of the flagellar helix, this anisotropic friction leads to a coupling of the rotation and translation of the helix, such that the rotation driven by the flagellar motor, results in a translational movement of the flagellum and with it of the cell body. The latter rotates in the opposite direction in order to balance the torques.

Within the description sketched so far and additional approximations for long and thin flagella, the following expression can be derived for the velocity of the bacterium [30]:

$$v \approx \alpha R \omega_m \times \left( \frac{\xi_\perp}{\xi_\parallel} - 1 \right) \times \frac{\xi_{\mathrm{rot}} R_b^3}{\xi_\perp R^2 L}. \tag{3}$$

The first term corresponds to an overall velocity scale, which depends on the pitch angle $\alpha$ and the radius $R$ of the helix (Fig. 2) as well as on the angular velocity $\omega_m$ of the motor. The term in the middle reflects the requirement for anisotropic friction, $\xi_\perp$ and $\xi_\parallel$ are the friction coefficients per unit length of a rod pulled perpendicular or parallel to the direction of its axis, respectively. This term is of order one, because $\xi_\perp \approx 2\xi_\parallel$ for long rods [30]. The last term expresses the dependence on the geometric parameters of the helix (Fig. 2) and corresponds to the ratio of the rotational friction

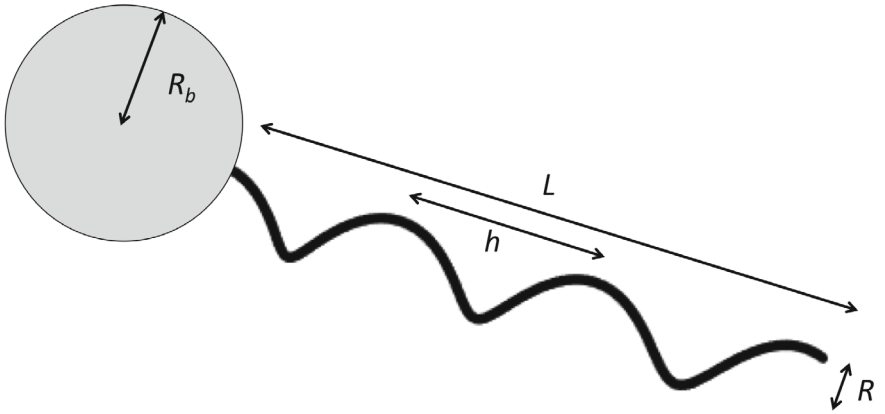


**Fig. 2.** A spherical bacterium with a single flagellum characterized by the radius $R$, the length $L$, and the pitch $h$. The pitch angle $\alpha$ is defined via $\tan\alpha = h/(2\pi R)$. The cell body has radius $R_b$.

of the cell body (taken as a sphere with radius $R_b$ and with friction coefficient $\xi_{\mathrm{rot}}$) and the perpendicular friction of the flagellar helix (with radius $R$ and length $L$).

Importantly, within the approximations made, the drag opposing the movement is entirely given by the flagellum, an increase in either its length or radius reduces the velocity. By contrast the size of the cell body increases the velocity, as its role is not to provide friction but rather to take up the counter-torque allowing the flagellum to rotate against the cell body. If the sense of rotation is changed, the direction of motion is reversed. However, at this point the flexibility of the flagella comes into play.

In general, the bacterium needs a mechanism to change direction. For bacteria with a single flagellum, it was recently shown that reversal of the sense of rotation of the flagellum leads to a buckling instability in the flagellum that reorients the cell [31]. The corresponding pattern of motion is called run-reverse-flick [32].

The case of bacteria with many flagella such as *Escherichia coli* is much better studied. The flagella of *E. coli* form a bundle and rotate collectively, powering directed motion, when their motors rotate counterclockwise. Upon clockwise rotation of one or more motors the bundle dissolves and individual flagella push the cell in different directions, resulting to a reorientation of the bacterium [28]. These reorientation events called tumbles have short durations and are the basis of a random walk motion called run-and-tumble, which is essential for chemotaxis (Sect. 6).

The idealized magnetotactic bacterium shown in Fig. 1 has two flagella, one at each pole, as it is the case in *M. gryphiswaldense*. When a bacterium reverses its direction of motion in the presence of a magnetic field, it keeps its orientation (due to magnetic alignment) rather than performing a U-turn. Thus, a turn can be accomplished by a change of the direction of rotation of both flagella, if they are active at the same time. Alternatively, it could be accomplished by a switch from one flagellum pushing (or alternatively pulling) the cell body to the other, if it is always the rear flagellum (respectively the front flagellum) that powers motion. The question how two flagella work together in such an organism has so far only been addressed in one study, which favors the second mechanism [33].

## 4 Directionality: Alignment in an external field

The total magnetic moment of a magnetotactic bacterium with a chain of 20 magnetosomes of size 50 nm as above is $6.2 \times 10^{-16}$ Am$^2$. Passive alignment of a magnetic

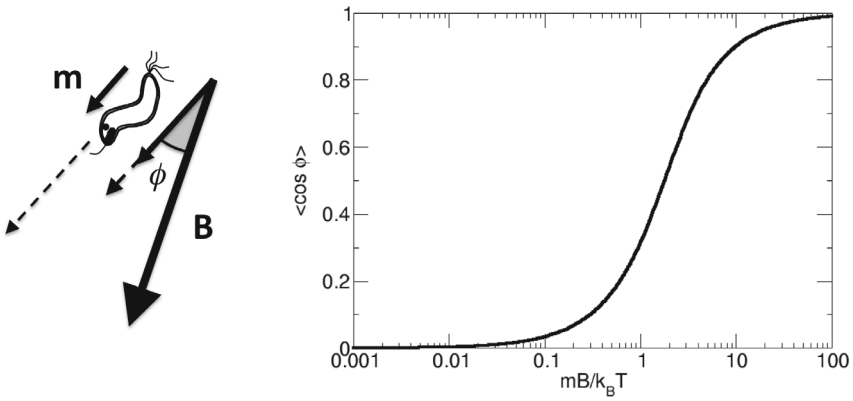


**Fig. 3.** Orientation of a magnetotactic bacterium with magnetic moment **m** in an external magnetic field **B**. The alignment of the cell body and the swimming direction deviates from the direction of the field by an angle $\phi$. This deviation is characterized by the Langevin function given in Eq. (5), however, typically with an effective temperature.

moment **m** in a (spatially homogeneous) magnetic field **B** is characterized by the energy

$$E = -\mathbf{m} \cdot \mathbf{B} = -mB \cos \phi. \tag{4}$$

In their natural habitat, the magnetic field is the field of the Earth with a strength of about $50\,\mu$T. Thus, alignment of the body axis of the bacterium with the field is characterized by an energy of $-3.1 \times 10^{-20}$ J or $-7.6\,k_BT$ (converting the units via T = J $A^{-1}m^{-2}$ and assuming room temperature with $k_BT = 4.1$ pN nm). Thus, a magnetic field of the strength of the Earth's field is in principle sufficient to passively align magnetotactic bacteria against thermal fluctuations and the magnetosome chain can indeed function as a compass needle. We note however that even though the alignment energy exceeds $k_BT$, it can be overcome by external forces or additional fluctuations such as vorticity of the water or non-thermal fluctuations arising from the active motion of the bacteria themselves. We will come back to this issue below.

Passive alignment with an external field is quantitatively characterized by the normalized average energy or the expectation value of $\cos\phi$, with $\phi$ being the alignment angle (Fig. 3). This value is given by the so-called Langevin function, which was originally derived for a paramagnet in an external field [34],

$$\langle \cos \phi \rangle = L\left(\frac{mB}{k_BT}\right) = \coth\left(\frac{mB}{k_BT}\right) - \frac{k_BT}{mB}. \tag{5}$$

The function is plotted in Fig. 3. The alignment of the bacteria and their trajectories with the magnetic field has been analyzed in several studies, which find that alignment is indeed described by Eq. (5), but only if a higher effective temperature is used [35,36]. The effective temperature values vary between studies and depend on the magnetic moment that is assumed (or inferred from electron microscopy images). An increased effective temperature indicates that alignment of the swimming direction is subject to fluctuations that are of non-thermal origin, likely due to the swimming of the bacteria. Consistent with this interpretation, one study found that alignment of the cell body with the field is better for dead bacteria than for swimming bacteria [37]. Two recent observations describe a dependence of the alignment on the physiological conditions. On the one hand, our own preliminary data (L. Landau et al., unpublished) indicate that the noise may depend on whether conditions are oxic or anoxic. On the other hand, a mutant of *M. magnetotacticum* lacking

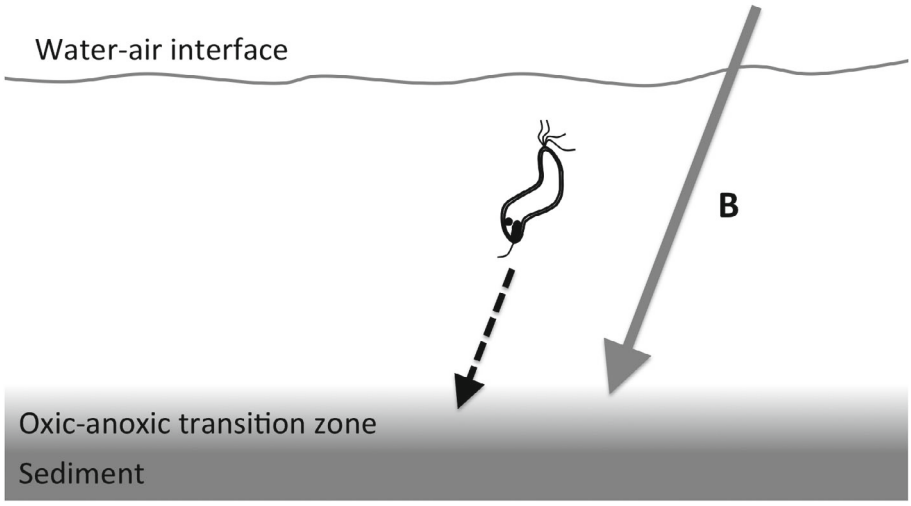


**Fig. 4.** Guidance of the swimming of a magnetotactic bacterium by the magnetic field of the Earth.

a chemotaxis gene showed a poorer alignment or an increased effective temperature compared to the wild type [38]. This was interpreted in terms of an active magnetosensory system, but since both strains exhibit fluctuations beyond thermal ones, the role of the corresponding gene could also be in the process that generates the non-thermal noise.

We note that in a homogeneous field, the field only orients the bacteria, but does not pull them. Thus, active swimming of the bacteria is required for directed motion, but the magnetic field defines the direction. Obviously, magnetotactic bacteria (or, for that matter, any other magnetic objects) could also be steered by a magnetic field that is not spatially homogeneous (e.g. with a bar magnet). In that case, the gradient of the magnetic field provides an attractive force that pulls the bacteria in addition to their swimming. Dead bacteria could be pulled in the same way. In a homogeneous field, however, dead bacteria only align, but do not move.

## 5 Magneto-aerotaxis

The role of magnetic navigation in bacteria becomes clearer if one considers that these bacteria are microaerophilic, i.e. grow best under conditions of low (but non-zero) oxygen concentration [39]. The preferred oxygen concentrations for magnetotactic bacteria are in the range of a 1–20 $\mu$M, low compared to a saturation concentration of oxygen in water of 216 $\mu$M [13]. Indeed, their natural habitat is the oxic-anoxic transition zone in layered aquatic environments, an area of great ecological diversity, which is typically located in the upper region of the sediment (mud) at the bottom of the water column [40]. As the magnetic field of the Earth has a vertical component (which points downwards on the Northern hemisphere), swimming along the field lines carries the bacteria towards the preferred habitat (Fig. 4). A layered (or stratified) water column is important for magnetotactic bacteria in two respects: It

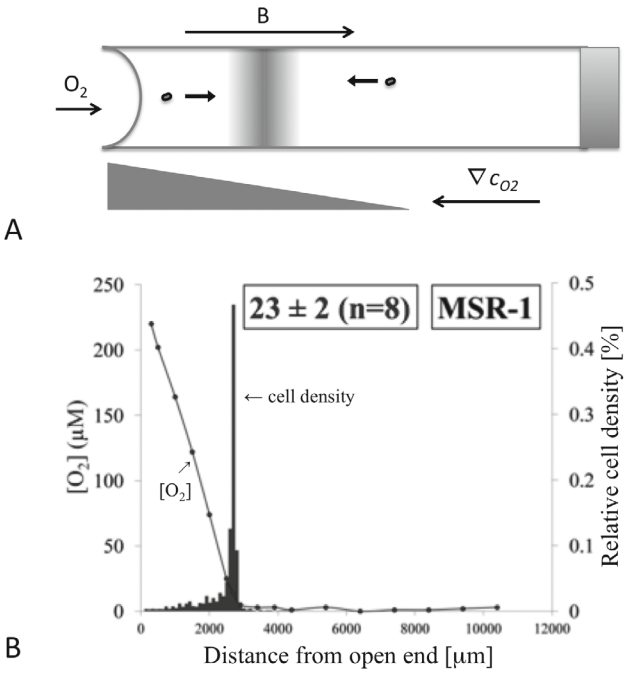


**Fig. 5.** Band formation in a capillary: (A) A capillary is closed at one end, but open at the other, allowing an oxygen gradient to build up. The magnetic field points towards the closed end. Magnetotatcic bacteria accumulate in a band at their preferred oxygen concentration. (B) Spatial profile of the oxygen concentration and the bacterial density for *M. gryphiswaldense* MSR-1 (from Ref. [13]).

allows an oxic-anoxic transition zone to form due to incomplete mixing in vertical direction. In addition, turnover of the water column (e.g. due to turbulent flow) would be detrimental to the orientation of the bacteria with respect to the magnetic field.

The situation found in the environment (without the sediment) can be recreated in the lab using the capillary assay (Fig. 5(A)): Magnetotactic bacteria are placed in a thin capillary that is open at one end, such that oxygen can be exchanged with the surrounding air, but closed at the other. The capillary is placed in a well-defined homogeneous magnetic field (with compensation of magnetic fields from the surrounding) and the dynamics of the bacterial density or of individual bacteria is then observed with a microscope [41].

An oxygen gradient builds up dynamically in the capillary due to oxygen diffusion and consumption by respiration of the bacteria. For a magnetic field pointing towards the closed end of the capillary (the anoxic side), the oxygen gradient is antiparallel to the magnetic field as in the natural habitats on the Northern hemisphere. Magnetotactic bacteria form a band in such a situation [13,41–43], i.e. a region of high bacterial density at a position where the local oxygen concentration corresponds to the preferred concentration. Individual bacteria perform excursions out of the band and back toward it. Figure 5(B) shows an example: a linear oxygen gradient and the density profile of bacteria, where the band is seen as a sharp peak.

Formation of such bands is common among bacteria that live in gradient environments, not only for oxygen, but also for gradients of other nutrients. Band formation in oxygen gradients is not specific to magnetotactic bacteria, but is also seen in non-magnetic species [44].

To test whether the bacteria are directed towards the preferred location, i.e. the band, by the oxygen gradient or by the magnetic field, the magnetic field can be reversed after the band has formed. Originally this experiment was done with the *Magnetospirilla* species that could be cultivated in the lab, the standard strains described above. For these bacteria, the band was stable after reversal of the field [42,43]. This observation indicates that the magnetic field is not used to bias the bacteria's swimming towards the band, but rather that it only defines an axis of motion. Effectively the field reduces the search for the location with the preferred oxygen concentration (which is guided by the oxygen gradient) from a three-dimensional search to a one-dimensional one. This behavior was therefore termed axial magneto-aerotaxis. A recent twist to this classical result is that the behavior of the Magnetospirilla upon field reversal is dependent on the conditions under which the culture has been grown. Grown under conditions closer to the natural ones, the magnetospirilla show a different behavior, namely polar magnetotaxis, discussed below, or a mixture of polar and axial magneto-aerotaxis [13,45].

A different response to the field reversal was observed later for another strain of magnetotactic bacteria, magnetotactic cocci, MC-1 [43]. These bacteria form a band just like the Magnetospirilla, but upon reversal of the field, they swim away from the location of the band in both directions. In our recent study comparing 12 different strains, this behavior was found to be the most frequent one (seen in 7 out of 12 strains) [13]. That the bacteria swim away from their preferred oxygen concentration clearly demonstrates that their motion is not directed by the oxygen gradient. Instead the direction of motion is determined by the magnetic field, which appears to function as a proxy for the oxygen gradient. Use of the magnetic field as a proxy is fine under natural conditions, where the field is antiparallel to the oxygen gradient, but results in persistent swimming in the wrong direction after field reversal. We note that even though the direction of swimming is independent of the gradient of the oxygen concentration, it does depend on the local oxygen concentration itself, as cells on the oxic and anoxic side of the band swim (predominantly) in opposite directions. Since the magnetic field determines the direction and polarity of motion, this behavior is called polar magnetotaxis (or dipolar magnetotaxis to distinguish it from the unipolar behavior described next).

In addition to these two behaviors, our comparison of different strains [13] showed several additional ones: In unipolar magnetoaerotaxis (seen for 3 out of 12 strains), upon field reversal the bacteria swim away from the location of the band in one direction only, oxic (two strains) or anoxic (one strain). In two cases, combinations of axial and polar or axial and unipolar behavior are seen, such that the band is retained by a subpopulation, while the rest of the population swims away. Whether the different behaviors of individual cells reflect differences in their individual histories such as previous exposure to an oxygen gradient or point towards a survival strategy (bet hedging) under unpredictable conditions (with conflicting environmental signal) is an open question. Unfortunately, so far no obvious correlation was found between the different magnetotactic behaviors and the morphology of the cells or their motility apparatus [13].

## 6 Modeling magneto-aerotaxis

Aerotaxis and magneto-aerotaxis can be seen as types of chemotaxis for oxygen and, thus, can be described mathematically in similar form (see Refs. [46,47] for introductions to chemotaxis). In the simplest case, the bacteria in the capillary can be described by one-dimensional dynamics [41,48,49], so that only two densities of bacteria, those swimming to the left and to the right, $\rho_L(x,t)$ and $\rho_R(x,t)$, respectively,

need to be considered. This description is valid for magnetotaxis when the magnetic field is parallel or antiparallel to the capillary axis (it can be used for other cases by considering the projection of the velocity). In addition, the oxygen concentration $c(x,t)$ is also dynamic, requiring a third equation. Thus, the full dynamics is given by

$$\frac{\partial \rho_L}{\partial t} = -v_L \frac{\partial \rho_L}{\partial x} - k_{LR}\rho_L + k_{RL}\rho_R \tag{6}$$

$$\frac{\partial \rho_R}{\partial t} = -v_R \frac{\partial \rho_R}{\partial x} + k_{LR}\rho_L - k_{RL}\rho_R \tag{7}$$

$$\frac{\partial c}{\partial t} = D\frac{\partial^2 c}{\partial x^2} - k(c)(\rho_L + \rho_R). \tag{8}$$

The first two equations describe the left- and right-swimming bacteria with terms for the drift velocity and for changes of direction. $v_L$ and $v_R$ are the velocities of the left- and right-swimming bacteria and $k_{LR}$ and $k_{RL}$ are the rates at which the direction of motion is changed (reversed). Both velocities and reversal rates can in principle depend on the oxygen concentration, the gradient of the oxygen concentration and the magnetic field. The third equation describes the diffusion of oxygen and its consumption by respiration of the bacteria. Here, $D$ is the diffusion coefficient of oxygen in water and $k(c)$ is the rate of respiration. A Michaelis-Menten dependence of the respiration rate on the oxygen concentration is assumed, $k(c) = k_{\max}c/(K+c)$, which makes sure that consumption of oxygen ceases when the oxygen concentration drops to zero. The following boundary conditions are used: The oxygen concentration is fixed at the saturated value at the left (open) end and the flux of bacteria through both ends of the capillary vanishes, as does the flux of oxygen at the right (closed) end.

The dynamics of the oxygen concentration is affected by the dynamics of the bacteria as the bacteria determine the spatial dependence of the oxygen consumption. For a sharp band at the preferred oxygen concentration $c^*$ of the bacteria, a linear oxygen concentration profile is obtained and the balance between the diffusive flux of oxygen to the band and oxygen consumption in the band sets the slope of the linear profile and thus the position of the band.

The dependence of the bacterial density on oxygen is more subtle and depends on the intracellular signal processing of the bacteria, which in turn is reflected in the parameter dependencies of $v_{L,R}(c, \partial_x c, B)$ and $k_{LR,RL}(c, \partial_x c, B)$. Here we will assume that the swimming speed is independent of the direction of motion ($v_R = -v_L$) and of the local oxygen concentration, as it is often the case for chemotactic motility. The paradigm for chemotactic motility is the run and tumble motion of *Escherichia coli*: These bacteria perform random walks consisting of phases of straight swimming (runs) and phases of rapid reorientation (tumbles) [47,50], as shown in Fig. 6. In a chemical gradient, runs are longer, when the bacterium swims up a gradient of a chemoattractant and shorter when it swims up a gradient of a repellent, which effectively biases the motion up or down the gradient, respectively. It is not clear whether magnetotactic bacteria make use of the run and tumble mechanism. As mentioned above, other strategies to generate (biased) random walks have been observed in other bacteria [51] as well as chemotactic eukaryotic cells [52,53]. Moreover, the average speed of some strains of magnetotactic bacteria is higher for bacteria swimming towards the band from the oxic side than the speed of bacteria swimming towards the band on the anoxic side and of bacteria swimming away from the band on either side [13,41], so the speed might contribute to biasing the swimming direction. Nevertheless, here we make a simplification and take the bias in the

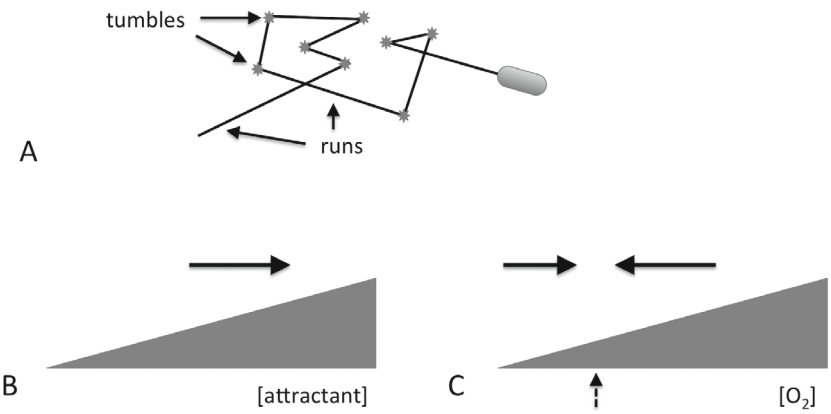


**Fig. 6.** Run and tumble motion in bacterial chemotaxis: (A) Bacterial random walk consisting of phases of straight swimming (runs) and phases of rapid reorientation (tumbles, indicated by stars). (B) The duration of runs is longer, when the bacterium swims against a gradient of a chemoattractant, biasing the random walk up the gradient. (C) In aerotaxis, the direction of the bias depends on whether the local oxygen concentration is larger or smaller than a preferred oxygen concentration, thus biasing the motion towards regions with the preferred oxygen concentration.

motion that guides the bacteria towards the band to be due to the reversal rates, as in the chemotaxis of *E. coli*.

In contrast to chemotaxis towards chemoattractors (such as food), here we have oxygen as an attractor at low concentration but as a repellent at high concentrations. Therefore, the switching rates must be different for oxygen concentrations higher and lower than the preferred concentration, $c^*$, which implies a dependence of the switching rates on the oxygen concentration in addition to a possible dependence on the gradient. The exact dependence on the oxygen concentration is unknown, so we assume a step-function dependence with just two values for the switching rates, a high and low value such that under normal conditions (magnetic field antiparallel to oxygen gradient) and with the open end to the left, $k_{LR}$ is high and $k_{RL}$ is low for at oxygen concentrations exceeding $c^*$. For $c < c^*$, the two values are switched. The second ingredient to describing a bias towards the band is a vectorial quantity that serves as directional reference. This quantity can be either the magnetic field (for polar magnetotaxis) or the oxygen gradient (for axial magnetotaxis or pure aerotaxis). Thus, the switching rates are obtained as

$$k_{LR} = \begin{cases} k_{\text{low}} & \text{for } c < c^* \text{ and } \boldsymbol{\nabla} c \cdot \boldsymbol{e}_x < 0 \\ k_{\text{high}} & \text{for } c < c^* \text{ and } \boldsymbol{\nabla} c \cdot \boldsymbol{e}_x > 0 \\ k_{\text{low}} & \text{for } c > c^* \text{ and } \boldsymbol{\nabla} c \cdot \boldsymbol{e}_x > 0 \\ k_{\text{high}} & \text{for } c > c^* \text{ and } \boldsymbol{\nabla} c \cdot \boldsymbol{e}_x < 0 \end{cases} \tag{9}$$

for the axial case and as

$$k_{LR} = \begin{cases} k_{\text{low}} & \text{for } c < c^* \text{ and } \boldsymbol{B} \cdot \boldsymbol{e}_x > 0 \\ k_{\text{high}} & \text{for } c < c^* \text{ and } \boldsymbol{B} \cdot \boldsymbol{e}_x < 0 \\ k_{\text{low}} & \text{for } c > c^* \text{ and } \boldsymbol{B} \cdot \boldsymbol{e}_x < 0 \\ k_{\text{high}} & \text{for } c > c^* \text{ and } \boldsymbol{B} \cdot \boldsymbol{e}_x > 0 \end{cases} \tag{10}$$

for the polar case. In these expressions $\boldsymbol{e}_x$ denotes a unit vector to the right. In all cases $k_{RL}$ has the opposite value (high/low) than $k_{LR}$.

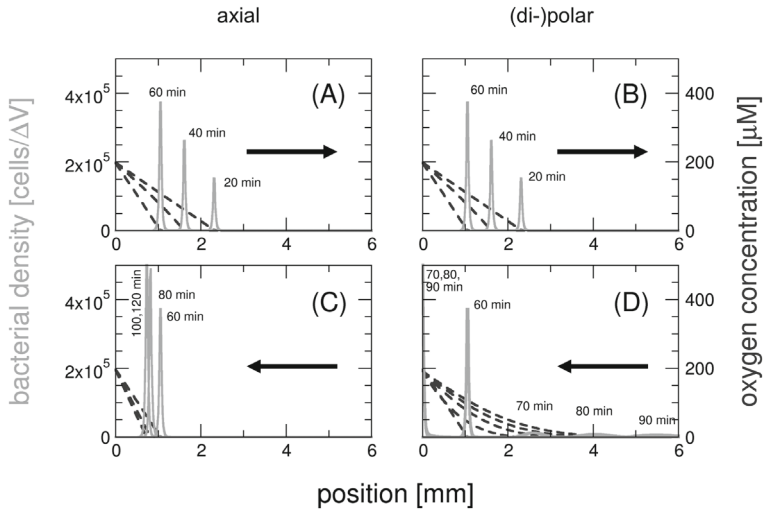


**Fig. 7.** Band formation in a model for magneto-aerotaxis in a capillary that is open at its left end ($x = 0$) and closed at the right end ($x = 40$ mm, not shown in the plots): (A,B) Formation of the band (peak in bacterial density, light grey) and the oxygen gradient (black dashed) via the axial and the polar mechanisms, starting at $t = 0$ with a homogeneous bacterial density and an initial oxygen gradient [13]. (C,D) Behavior of the band after reversal of the magnetic field (indicated by the arrows). In all four plots, the bacterial density is shown at discrete times, indicated by the labels next to the peaks of the bacterial density; the corresponding curve for the oxygen gradient is the one approaching zero in close proximity to that peak.

Equations (6)–(8) describe the formation of the band as well as its behavior after the magnetic field is switched (Fig. 7). Notably, a sharp band forms rather quickly at a position that depends on the initial conditions (in particular the oxygen concentration in the capillary) and then moves towards the stationary position. In Fig. 7, there is initially no oxygen in the capillary and the bacteria are homogeneously distributed. The slight movement of the band toward the open end (which is seen to continue a bit after field reversal) is due to the increase in the number of bacteria in the band, which leads to increased oxygen consumption, which in turn requires a steeper gradient for the balance of oxygen supply (by diffusion) and consumption. If the initial oxygen concentration in the system is high, two bands form that move in opposite directions, consuming the excess oxygen. One band will eventually reach the closed end of the capillary and then dissolve. With the reversal rates given by Eq. (9), the band is independent of the direction of the magnetic field and therefore stable against field reversal. With the rates from Eq. (10), the bacterial density follows the field and the bias of motion is reversed with the reversal of the field, resulting in two bands that move away toward both ends of the capillary, getting broader on the way. In this case, the oxygen gradient does not affect the reversal rates and thus the directional bias of the motion. Rather the magnetic field serves as a proxy for the oxygen gradient and following the field replaces gradient sensing.

Unipolar behavior is obtained in the model when the reversal rates depend on the direction of the oxygen gradient on one side of the band and on the magnetic field on the other. Such a model would be appropriate if two separate sensing systems for oxygen gradients are in place and used at high and low oxygen concentration, respectively, that can individually be replaced by following the magnetic field as a proxy. Identifying these sensing systems is a task for future work. So far, little is known about the sensors and signals underlying magnetotaxis. One notable exception is the

recent identification of an essential chemotaxis operon in *M. gryphiswaldense* [45]. The observation of poorer alignment with the external field in a mutant has also been interpreted to indicate a role for the deleted gene in sensing [38], but other interpretations remain possible, as discussed above.

To conclude this section, we note that in the discussion above, we have described magneto-aerotaxis as a one-dimensional process. Within this approach, an angle between the magnetic axis and the capillary axis (along which the gradient builds up) can be included by considering the projection of the magnetic field on the capillary axis [41]. For a full three-dimensional description, one also has to consider the alignment of the bacteria with the field, and in particular the deviations from perfect alignment. In some cases, such deviations are crucial, for example to sense an oxygen gradient if the magnetic field is perpendicular to the gradient (as it is the case at the equator) or to circumvent obstacles, a situation that is typical for cells living in the sediment [54].

## 7 From magnetotactic bacteria to synthetic magnetic microswimmers

The swimming of bacteria has long served as an inspiration for the design of synthetic or hybrid (partly biological, partly synthetic) microswimmers [55]. Specifically, magnetic fields provide an attractive mechanism for steering swimmers in a technological context as magnetic fields are easily applied externally. Thus in principle, any magnetic particle that is provided with a mechanism of propulsion could perform "magnetotactic" motion and move along field lines of a (spatially homogeneous) magnetic field. This principle has been employed in hybrid swimmers where a (non-magnetic) bacterium is attached to a magnetic particle [56]. We note that while steering a single particle (or many particles going in the same direction) is simple with such systems, steering multiple particles on independent trajectories is more difficult, because the external magnetic field cannot address individual particles, but affects all of them.

In addition to providing directionality, magnetic fields can also be used for propulsion. Specifically, spatially homogeneous, but rotating magnetic fields have been used to propell magnetic particles with helical shape resembling bacterial flagella (chiral swimmers or micro-/nanopropellers) [57,58]. While such particles are not strictly autonomous swimmers, they are also not subject to an external force that drives them. Rather, via their translation-rotation coupling, they convert an external torque into a translational motion. Even though this mechanism of propulsion has first been used for helical particles, the helical shape is not necessary, but a chirality of the shape is. In fact, recent work of our groups has shown that rapid propulsion can be achieved by selecting good swimmers from a population of particles with random shapes [59]. The fastest swimmers selected in this way exhibited speeds comparable to or even exceeding those of designed magnetic microswimmers [60]. (Since speeds are trivially proportional to particle size and actuation frequency, dimensionless speeds were used for that comparison by normalizing the observed speeds with the particle size and the rotation frequency of the field.) Mathematical optimization of the shape of helical microswimmers for rapid propulsion has shown that slender helices with a pitch comparable to their length should swim fastest [61]. Indeed some of the best propellers selected from the random shapes show a weak resemblance to such slender helices. Propellers with helical shape as well as random shapes can only follow the rotation of the magnetic field up to a critical rotation frequency, for which the maximal speed is obtained [59,62]. If the field is rotated with a frequency exceeding this critical frequency, the propeller rotates with a smaller frequency and therefore also moves with reduced speed. Due to that nonlinear dependence of the speed on the actuation

frequency, propellers with different critical frequencies can be steered independently by using multiple actuation frequencies [63,64]. The optimal strategy of control, for minimizing control time as well as the amount of required excursions away from the desired path, is to use the critical frequencies [64].

## 8 Concluding remarks

In summary, magnetotactic bacteria provide an interesting model system to study the role of physical forces in biological function. Importantly, the physical forces can provide new functions, but, at same time, they come with their intrinsic constraints that other cellular processes may have to deal with. Here, a good example is cell division, where attractive magnetic forces must be overcome [19] and the magnetic organization must be preserved in both daughter cells [65]. Swimming of these bacteria is subject to magnetic orientation, which allows to steer them to their preferred habitat, the oxic-anoxic transition zone, as (on the Northern hemisphere) the oxygen gradient in aquatic environments and the magnetic field are antiparallel. Interestingly, the largest fraction of the strains studied follows the magnetic field rather than sensing the oxygen gradient, suggesting that such proxy use is advantageous in some way. One can speculate that the magnetic field is the preferred directional clue because it is more stable and not perturbed by water movements as the gradient of the concentration of dissolved oxygen.

This minireview is an extended and revised version of our lecture notes for the DFG SPP 1726 summer school 2015 in Jülich [66]. The authors acknowledge support by the DFG priority program SPP 1726 “Microswimmers – from single particle motion to collective behavior” (grant No. FA 835/7-1 and KL 818/2-1) and by the European Research Council through Starting Grant 256915-MB2 (to D.F.).

## References

1. M. Winklhofer, Phys. unserer Zeit **35**, 120 (2004)
2. D.A. Bazylinski, R.B. Frankel, Nat. Rev. Microbiol. **2**, 217 (2004)
3. D. Faivre, D. Schuler, Chem. Rev. **108**, 4875 (2008)
4. S. Bellini, *Su di un particolare comportamento di batteri d’acqua dolce*, Instituto di Microbiologia dell’Universita di Pavia (1963)
5. R.P. Blakemore, Science **190**, 377 (1975)
6. R.B. Frankel, R.P. Blakemore, R.S. Wolfe, Science **203**, 1355 (1979)
7. C.T. Lefèvre, D.A. Bazylinski, Microbiol. Mol. Biol. Rev. **77**, 497 (2013)
8. T. Matsunaga, A. Arakaki, in *Magnetoreception and Magnetosomes in Bacteria*, edited by D. Schüler (Springer, Berlin, 2007), p. 227
9. A. Komeilli, FEMS Microbiol. Rev. **36**, 232 (2012)
10. D. Faivre, MRS Bull. **40**, 509 (2015)
11. C.T. Lefevre, M. Bennet, S. Klumpp, D. Faivre, in preparation
12. S. Mann, N.C.H. Sparks, R.B. Frankel, D.A. Bazylinski, H.W. Jannasch, Nature **343**, 258 (1990)
13. C.T. Lefèvre, M. Bennet, L. Landau, P. Vach, D. Pignol, D.A. Bazylinski, R.B. Frankel, S. Klumpp, D. Faivre, Biophys. J. **107**, 527 (2014)
14. K. Schleifer, D. Schüler, S. Spring, M. Weizenegger, R. Amann, W. Ludwig, M. Köhler, Syst. Appl. Microbiol. **14**, 379 (1991)
15. A. Körnig, M. Winklhofer, J. Baumgartner, T.P. Gonzalez, P. Fratzl, D. Faivre, Adv. Funct. Mat. **24**, 3926 (2014)
16. D.J. Dunlop, Ö. Özdemir, *Rock Magnetism: Fundamentals and Frontiers* (Cambridge University Press, New York, 1997)

17. J. Howard, *Mechanics of Motor Proteins and the Cytoskeleton* (Sinauer, Sunderland MA, 2001)
18. S.S. Staniland, C. Moisescu, L.G. Benning, J. Basic Microbiol. **50**, 392 (2010)
19. E. Katzmann, F.D. Muller, C. Lang, M. Messerer, M. Winklhofer, J.M. Plitzko, D. Schuler, Mol. Microbiol. **82**, 1316 (2011)
20. S. Ullrich, M. Kube, S. Schübbe, R. Reinhardt, D. Schüler, J. Bacteriol. **187**, 7176 (2005)
21. D. Faivre, L.H. Böttger, B.F. Matzanke, D. Schüler, Angew. Chem. Int. Ed. **46**, 8495 (2007)
22. D. Faivre, A. Fischer, I. Garcia-Rubio, G. Mastrogiacomo, A.U. Gehring, Biophys. J. **99**, 1268 (2010)
23. S. Klumpp, D. Faivre, PLoS One **7**, e33562 (2012)
24. A. Komeili, Z. Li, D. Newman, G.J. Jensen, Science **311**, 242 (2006)
25. A. Scheffel, M. Gruska, D. Faivre, A. Linaroudis, J.M. Plitzko, D. Schuler, Nature **440**, 110 (2006)
26. B. Kiani, D. Faivre, S. Klumpp, New J. Phys. **17**, 043007 (2015)
27. E. Katzmann, A. Scheffel, M. Gruska, J.M. Plitzko, D. Schuler, Mol. Microbiol. **77**, 208 (2010)
28. H.C. Berg, Physics Today **53**, 24 (2000)
29. R.G. Winkler, Eur. Phys. J. Special Topics **225**, 2079 (2016)
30. E. Lauga, T.R. Powers, Rep. Prog. Phys. **72**, 096601 (2009)
31. K. Son, J.S. Guasto, R. Stocker, Nat. Phys. **9**, 484 (2013)
32. L. Xie, T. Altindal, S. Chattopadhyay, X.-L. Wu, Proc. Natl. Acad. Sci. USA **108**, 2246 (2011)
33. D. Murat, M. Hzrisse, L. Espinosa, A. Bossa, F. Alberto, L.-F. Wu. J. Bacteriol. **197**, 3275 (2015)
34. P. Langevin, J. Phys. Theor. Appl. **4**, 678 (1905)
35. A.J. Kalmijn, IEEE Trans. Magnetics **17** (1981)
36. R. Nadkarni, S. Barkley, C. Fradin, PLoS One **8**, e82064 (2013)
37. C. Rosenblatt, F.F. Torres de Araujo, R.B. Frankel, Biophys. J. **40**, 83 (1982)
38. X. Zhu, G. Xin, L. Ning, L.-F. Wu, C. Luo, Q. Ouyang, Y. Tu, G. Chen, Integr. Biol. **6**, 706 (2014)
39. U. Heyen, D. Schüler, Appl. Microbiol. Biotechnol. **61**, 536 (2003)
40. A. Brune, P. Frenzel, H. Cypionka, FEMS Microbiol. Rev. **24**, 691 (2000)
41. M. Bennet, A. McCarthy, D. Fix, M.R. Edwards, F. Repp, P. Vach, J.W.C. Dunlop, M. Sitti, G.S. Buller, S. Klumpp, D. Faivre, PLoS One **9**, e101150 (2014)
42. A.M. Spormann, R.S. Wolfe, FEMS Microbiol. Lett. **22**, 171 (1984)
43. R.B. Frankel, D.A. Bazylinski, M.S. Johnson, B.L. Taylor, Biophys. J. **73**, 994 (1997)
44. I.B. Zhulin, V.A. Bespalov, M.S. Johnson, B.L. Taylor, J. Bacteriol. **178**, 5199 (1996)
45. F. Popp, J.P. Armitage, D. Schüler, Nat. Commun. **5**, 5398 (2014)
46. G.H. Wadhams, J.P. Armitage, Nat. Rev. Mol. Cell Biol. **5**, 1024 (2004)
47. V. Sourjik, N.S. Wingreen, Curr. Opin. Cell Biol. **24**, 262 (2012)
48. B.C. Mazzag, I.B. Zhulin, A. Mogilner, Biophys. J. **85**, 3558 (2003)
49. M.J. Smith, P.E. Sheehan, L.L. Perry, K. O'Connor, L.N. Csonka, B.M. Applegate, L.J. Whitman, Biophys. J. **91**, 1098 (2006)
50. H.C. Berg, D.A. Brown, Nature **239**, 500 (1972)
51. L. Xie, T. Altindal, S. Chattopadhyay, X.-L. Wu, Proc. Natl. Acad. Sci. USA **108**, 2246 (2011)
52. R. Jeanneret, M. Contino, M. Polin, Eur. Phys. J. Special Topics **225**, 2141 (2016)
53. U.B. Kaupp, L. Alvarez, Eur. Phys. J. Special Topics **225**, 2119 (2016)
54. X. Mao, R. Egli, N. Petersen, M. Hanzlik, X. Liu, PLoS One **9**, e102810 (2014)
55. M. Sitti, Nature **458**, 1121 (2009)
56. R.W. Carlsen, M.R. Edwards, J. Zhuang, C. Pacoret, M. Sitti, Lab Chip **14**, 3850 (2014)
57. A. Ghosh, P. Fischer, Nano Lett. **9**, 2243 (2009)
58. M. Alarcón-Correa, D. Walker, T. Qiu, P. Fischer, Eur. Phys. J. Special Topics **225**, 2241 (2016)

59. P.J. Vach, N. Brun, M. Bennet, L. Bertinetti, M. Widdrat, J. Baumgartner, S. Klumpp, P. Fratzl, D. Faivre, Nano Lett. **13**, 5373 (2013)
60. P.J. Vach, P. Fratzl, S. Klumpp, D. Faivre, Nano Lett. **15**, 7064 (2015)
61. E.E. Keaveny, S.W. Walker, M.J. Shelley, Nano Lett. **13** 531 (2013)
62. D. Schamel, M. Pfeifer, J.G. Gibbs, B. Miksch, A.G. Mark, P. Fischer, J. Am. Chem. Soc. **135**, 12353 (2013)
63. A.W. Mahoney, N.D. Nelson, K.E. Peyer, B.J. Nelson, J.J. Abbott, Appl. Phys. Lett. **104**, 144101 (2014)
64. P.J. Vach, S. Klumpp, D. Faivre, J. Phys. D: Appl. Phys. **49**, 065003 (2016)
65. C.T. Lefèvre, M. Bennet, S. Klumpp, D. Faivre, mBio **6**, e02286 (2015)
66. S. Klumpp, D. Faivre, in *Microswimmers – From Single Particle Motion to Collective Behaviour. Lecture Notes of the DFG SPP 1726 Summer School 2015*, edited by G. Gompper et al. (Forschungszentrum Jülich, 2015), Chap. B.5